



DYNA

ISSN: 0012-7353

ISSN: 2346-2183

Universidad Nacional de Colombia

Rodrigues, Jozé André de Moraes; Lopes, Fabrício Marcos Oliveira; Silva, Jhon
Lennon Bezerra da; Araújo, Hélio Lopes; Silva, Marcos Vinícius da; Santos,
Anderson dos; Batista, Pedro Henrique Dias; Moura, Geber Barbosa de Albuquerque
Spatial-temporal dynamics of Caatinga vegetation cover by remote sensing in the Brazilian semiarid region
DYNA, vol. 87, no. 215, 2020, October-December, pp. 109-117
Universidad Nacional de Colombia

DOI: <https://doi.org/10.15446/dyna.v87n215.87851>

Available in: <https://www.redalyc.org/articulo.oa?id=49668129013>

- How to cite
- Complete issue
- More information about this article
- Journal's webpage in redalyc.org

UNAM 

Scientific Information System Redalyc
Network of Scientific Journals from Latin America and the Caribbean, Spain and
Portugal

Project academic non-profit, developed under the open access initiative

Spatial-temporal dynamics of Caatinga vegetation cover by remote sensing in the Brazilian semiarid region

Joez André de Moraes Rodrigues^a, Pabrcio Marcos Oliveira Lopes^b, Jhon Lennon Bezerra da Silva^a, Hélio Lopes Araújo^a, Marcos Vinicius da Silva^c, Anderson dos Santos^a, Pedro Henrique Dias Batista^c & Geber Barbosa de Albuquerque Moura^b

^a Department of Agricultural Engineering, Federal Rural University of Pernambuco, Recife, Pernambuco, Brazil. joezandre@hotmail.com; jhonlennoigt@hotmail.com; heliopiassaba@gmail.com; agryanderson@gmail.com

^b Department of Agronomy, Federal Rural University of Pernambuco, Recife, Pernambuco, Brazil. pabriciope@gmail.com; geber.moura@ufrpe.br

^c Department of Ambience, Federal Rural University of Pernambuco, Recife, Pernambuco, Brazil. marcolino_114@hotmail.com; giga_pedro@hotmail.com

Received: May 30th, 2020. Received in revised form: August 21th, 2020. Accepted: September 8th, 2020

Abstract

The Brazilian semiarid region is marked by water scarcity, which causes the loss of leaves from native vegetation to reduce transpiration. With the reduction of the Caatinga leaf area, the soil becomes more exposed, which makes it a great ally for environmental degradation. This study aimed to monitor and analyze the spatial-temporal dynamics of the Caatinga vegetation by orbital remote sensing in the semiarid region of Pernambuco, Brazil, in the rainy and dry season. The study was developed from Landsat-8 satellite images between the years 2013-2018. From the SEBAL algorithm, thematic maps of the biophysical parameters were determined: albedo and surface temperature, normalized difference vegetation index (NDVI), soil-adjusted vegetation index (SAVI), and leaf area index (LAI). The results show that in the dry season, there is a greater aptitude for environmental degradation to occur.

Keywords: environmental monitoring; surface temperature; Landsat-8; albedo.

Dinámica espacio-temporal de la cubierta vegetal de la Caatinga por teledetección orbital en la región semiárida del Brasil

Resumen

La región semiárida brasileña se caracteriza por la escasez de agua, lo que provoca la pérdida de hojas de la vegetación nativa para reducir la transpiración. Con la reducción del área foliar de Caatinga el suelo está más expuesto, convirtiéndose en un gran aliado para la degradación ambiental. El objetivo fue vigilar y analizar la dinámica espacio-temporal de la vegetación de Caatinga mediante la teledetección orbital en región semiárida de Pernambuco, Brasil, en la estación de lluvias en la estación seca. Estudio se desarrolló mediante imágenes del satélite Landsat-8, entre los años 2013-2018, y mediante el algoritmo SEBAL se determinaron mapas temáticos de los parámetros biofísicos: albedo y temperatura superficial, índice de vegetación de diferencia normalizada (NDVI), índice de vegetación ajustado al suelo (SAVI) e índice de área foliar (LAI). Los resultados muestran que en la estación seca hay una aptitud más notable para que se produzca la degradación ambiental.


Palabras clave: vigilancia ambiental; temperatura de la superficie; Landsat-8; albedo.

1. Introduction

The Brazilian semiarid region had an increase in its area of extension, current processing 1.127.953 km², of which almost 90% are mainly in the northeast region of Brazil, that

is, 1.006.738 km², the other part being located in the north of the state of Minas Gerais [13]. This new demarcation was based on the 800-mm annual isohyet and the Thornthwaite aridity index [26] below 0.50, and the drought risk above 60% was also considered.

How to cite: Rodrigues, J.A.M, Lopes, P.M.O, Silva, J.L.B, Araújo, H.L, Silva, M.V, Santos, A, Batista, P.H.D. and Moura, G.B.A. Spatial-temporal dynamics of Caatinga vegetation cover by remote sensing in the Brazilian semiarid region. DYNA, 87(215), pp. 109-117, October - December, 2020.

© The author; licensee Universidad Nacional de Colombia. 
Revista DYNA, 87(215), pp. 109-117, October - December, 2020., ISSN 0012-7353
DOI: <http://doi.org/10.15446/dyna.v87n215.87851>

In the semiarid region of Brazil, the climate stands out, since the annual rainfall averages are closely linked to the local economy and to the vegetation, besides the formation and changes in the soil [27]. Remember that in these places, there is always a poor distribution of rainfall, where the dry periods are usually prolonged. The rainy periods generally occur between February and May, with poorly distributed precipitation, high intensity, and short duration [9].

The predominant vegetation in this region is the Caatinga biome, which represents 11% of the national territory, which corresponds to 844,453 km², being the most representative ecosystems of the northeast of the country and the north of the state of Minas Gerais [13]. This type of vegetation is highly sensitive to climate change, having a rapid production of plant biomass from the onset of rains. On the other hand, in the dry season, the Caatinga loses its leaves, a defense mechanism, being possible the clear perception of reduction of the vegetal biomass and leaf area of plants of this ecosystem [6,8,22,23].

Another important aspect of the natural condition of environmental changes in the Caatinga due to drought events is the anthropic action in this type of biome, as well as the conditions of climate change accelerate the processes of environmental degradation of native vegetation. Since this vegetation needs long periods to recover when not in a desertification environment. The Satellite Image Analysis and Processing Laboratory/Federal University of Alagoas (LAPIS/UFAL) warn that due to these factors, about 62% of the areas susceptible to desertification in the country are in Caatinga, mainly in the semiarid regions of Brazil, directly affecting its fauna and flora with the extinction of endemic species and in general the biodiversity of the natural environment, as well as the scarcity of water and food, compromising the local socioeconomic conditions [5,16].

The spatial-temporal environmental monitoring of the Brazilian semiarid region shows itself as a strong ally in the prevention of the destruction of native vegetation, as well as for proposing measures for the recovery of the Caatinga biome [22,23]. Given the huge territorial extension of the region covered by Caatinga in Brazil, the monitoring of these areas requires techniques capable of providing quick and efficient responses to environmental changes, whether caused by bad weather or human action and even by the combination of these. With this in mind, the use of geoprocessing together with remote orbital sensing techniques, mainly for the evaluation of plant biomass and leaf area through vegetation indices and biophysical parameters such as albedo and surface temperature, which highlight the condition of degraded areas or areas in the process of degradation, is essential due to practicality and low operational cost [7,24,22,23].

The orbital remote sensing has several techniques of worldwide use in researches involving the environment. One can highlight mainly the application of the Surface Energy Balance Algorithm for Land (SEBAL) algorithm that obtains information from the radiation and energy balance of the earth's surface, requiring only a few data, such as orbits and surface weather data [7,1,21,22,23].

Therefore, as the Caatinga is a biome of rapid responses to climate change and/or anthropic interference, this research aims to monitor and analyze the spatial-temporal dynamics of the Caatinga vegetation through orbital remote sensing techniques in determining biophysical parameters of the energy balance of earth surface, in Pesqueira, semiarid region of the state of Pernambuco, in the rainy and dry season, between the years 2013 to 2018.

2. Material and methods

2.1. Field of study

The area of this study is located in Pesqueira, inserted in the Upper Ipanema watershed, in the state of Pernambuco, semiarid region of Brazil. It is specifically located between the latitudes of 8°12'30" S and 8°38'30" S, and between the longitudes of 36°30' W and 36°58' W, with an altitude of 654 m (Fig. 1).

Fig. 1 illustrates the spatial map of the study area from an image of the Landsat-8 satellite, with 30 m spatial resolution. The image was georeferenced by the Geographic Coordinate System, DATUM: WGS1984 - Zone 24 South.

As a semiarid region, the municipality has a climate classified as BSh'w' according to Köppen [3]. According to [17], the annual average temperature and precipitation are 23 °C and 607 mm, respectively, and potential evapotranspiration of 2000 mm by year. The aridity index elaborated by [26] is less than 0.50 [13], confirming the Köppen classification, that is, semiarid and hot climate. The vegetation cover of the region presents itself with different densities and pastures, Caatinga being the predominant vegetation [18]. Moreover, according to [11], Pesqueira has several types of soils: Ultisol, Cambisol, Fluvisol, Leptosol, Regosol, and Planosol.

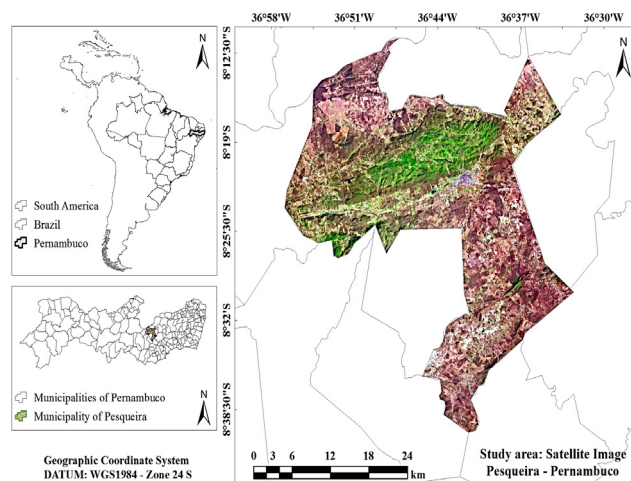


Figure 1. Spatial location of the study area, in Pesqueira, Pernambuco, Brazil.

Source: The Authors.

2.2. Weather data

Table 1 shows the monthly and annual rainfall collected by the Instituto Nacional de Meteorologia – Brazil [4], for the years of satellite image collection: 2013, 2015, and 2018. The year 2013 had the highest accumulated precipitation; however, the rains started in the second half of April and ended in early August; the precipitation was normal and poorly distributed (NPD) and outside the rainy season. In 2015, rainfall was low, characterizing it as a drier year (DY) than the others. However, the year 2018 was of regular and well-distributed rain (NWD), being mostly in the rainy season.

Table 2 also presents the instantaneous surface weather data collected by the Instituto Nacional de Meteorologia – Brazil [4]. The weather surface variables were the average air temperature (T_{air} , °C), relative air humidity (RH, %), and atmospheric air pressure (P_o , kPa). There are also the accumulated 90 days before the dates of the passage of the satellite. The previous rains for the years 2015 and 2018 were significantly greater than in 2013.

Table 1.
Monthly and annual rainfall and rainfall classification.

| Month | Rainfall (mm) | | |
|-----------|---------------|-------|-------|
| | 2013 | 2015 | 2018 |
| January | 5.0 | 18.0 | 23.2 |
| February | 0.0 | 64.3 | 52.7 |
| March | 2.0 | 3.7 | 53.8 |
| April | 127.8 | 54.2 | 96.5 |
| May | 14.5 | 5.0 | 67.4 |
| June | 83.2 | 59.2 | 26.9 |
| July | 166.8 | 70.1 | 12.8 |
| August | 25.5 | 30.6 | 31.7 |
| September | 8.0 | 7.2 | 0.0 |
| October | 15.0 | 2.4 | 55.0 |
| November | 17.0 | 0.0 | 16.4 |
| December | 46 | 21 | 20.7 |
| Total | 510.8 | 335.7 | 457.1 |
| Situation | NPD | DY | NWD |

Source: The Authors.

Table 2.
Surface weather data recorded during the passage of the Landsat-8 OLI/TIRS satellite.

| Image date | T_{air} (°C) | RH (%) | P_o (kPa) | Accumulated precipitation (mm) in the 90 days before the satellite's passage |
|------------|-------------------|-----------|----------------|------------------------------------------------------------------------------------------|
| | | | | |
| 04/14/2013 | 31.1 | 28.0 | 93.67 | 22.5 |
| 10/12/2013 | 28.2 | 31.0 | 93.85 | 37.0 |
| 04/04/2015 | 25.7 | 73.8 | 93.95 | 86.0 |
| 11/15/2015 | 27.2 | 59.0 | 93.98 | 12.4 |
| 05/14/2018 | 23.0 | 84.7 | 93.88 | 240.0 |
| 12/08/2018 | 26.4 | 73.5 | 93.96 | 79.4 |

Source: The Authors.

2.3. Orbital satellite data (Remote sensing - SEBAL)

The study was conducted using six orbital images of the Landsat-8 satellite with the sensors Operational Land

Imager/Thermal Infrared Sensor (OLI/TIRS), acquired through the United States Geological Survey (USGS) belonging to the National Aeronautics and Space Administration (NASA) space database. For this purpose, the images were divided into two groups: one from the rainy seasons on 04/14/2013, 04/04/2015, and 05/14/2018, and the other group from the dry season on 10/12/2013, 11/15/2015, and 12/08/2018.

The images were digitally processed in the ERDAS IMAGINE® 9.1 software, in which the Surface Energy Balance Algorithm for Land (SEBAL) algorithm was implemented, whose methodology was following [7] and [2]. From this algorithm, the grey levels of the images were converted into spectral radiance and monochromatic reflectance, which enabled the estimates of vegetation, albedo, and surface temperature indices.

The spectral radiance for the multispectral bands of the Landsat-8 satellite with the OLI sensor was determined by eq. (1).

$$L_b = Add_{rad} + Mult_{rad} \times ND_b \quad (1)$$

where: L_b - spectral radiance in each band ($W m^{-2} sr^{-1} \mu m^{-1}$); Add_{rad} - additive radiance terms; $Mult_{rad}$ - multiplicative radiance terms; ND_b - pixel intensity in each multispectral band (digital number between 0 and 65,535 grey levels).

Using eq. (2) [10,21] it was possible to calculate the monochromatic reflectance.

$$r_b = \frac{(Add_{ref} + Mult_{ref} \times ND_b)}{\cos \theta \times d_r} \quad (2)$$

where: r_b - monochrome reflectance in each band ($W m^{-2} sr^{-1} \mu m^{-1}$); Add_{rad} - additive terms relative to reflectance; $Mult_{rad}$ - multiplicative terms relative to reflectance; θ - solar zenith angle; d_r - square of the ratio of average and instantaneous distances between the earth and the sun on a given day of the year.

According to [15], the squared ratio between the mean and instantaneous distances between the Earth and the Sun on a given day of the year (d_r) is calculated by eq. (3).

$$d_r = 1 + 0.033 \times \cos\left(\frac{SDY \times 2 \times \pi}{365}\right) \quad (3)$$

where: SDY - the sequential day of the year, the argument of the \cos function in radians.

For the determination of the solar zenith angle (θ), the eq. (4) was used, from the angle of elevation of the sun for all images.

$$\theta = \cos\left(\frac{\pi}{2} - E\right) = \sin(E) \quad (4)$$

where: E - the angle of elevation of the sun.

The multispectral reflective bands from the OLI sensor Landsat-8 satellite images served to determine the NDVI and

SAVI vegetation indexes. These indexes range from -1 to 1, where the closer to 1, the greater the indication of vegetative activity, which indicates strong chlorophyll activity. The negative values of these generally indicate areas of water bodies. Values close to and in the range of zero indicate areas with little or no vegetation, of little or no chlorophyll activity, eq. (5) [8,2].

$$NDVI = \frac{r_{bIV} - r_{bV}}{r_{bIV} + r_{bV}} \quad (5)$$

where: r_{bIV} - infrared-reflective band; r_{bV} - red reflective band.

The SAVI determines to mitigate the antecedent effects of soil using an adjustable constant, eq. (6) [2].

$$SAVI = \frac{(1 + L) \times (r_{bIV} - r_{bV})}{(L + r_{bIV} + r_{bV})} \quad (6)$$

where: L - adjustment factor to soil conditions. The variation of the soil fit constant (L) is between 0 and 1, where usually 1 is used in processing areas with mild vegetation. For areas with intermediate ground cover, the adjustment factor of 0.5 is used. For areas with denser vegetation cover, it is recommended to use the adjustment factor of 0.25, and for a value of L equal to zero, the SAVI becomes similar to the NDVI; that is, there is no adjustment [12,1]. Due to the region of study belonging to the Brazilian semiarid region, the adjustment factor of 0.5 was utilized [24,22].

The leaf area index was also calculated from the SAVI according to the work of [22], also in a region of the Brazilian semiarid. This parameter is represented by the ratio between the leaf area of the canopy and the surface moisture projected on the soil, as shown in eq. (7) [1].

$$LAI = - \frac{\ln\left(\frac{0.69 - SAVI}{0.59}\right)}{0.91} \quad (7)$$

where: LAI ($m^2 m^{-2}$) - leaf area index.

The surface albedo was based on studies mainly developed in semiarid regions of Brazil, determined according to eq. (8) [2,21,23].

$$\alpha_{sur} = \frac{\alpha_{toa} - \alpha_{atm}}{\tau_{sw}^2} \quad (8)$$

where: α_{sur} - surface albedo; α_{toa} - planetary albedo based on the weight coefficients suggested for the OLI sensor by [21]; α_{atm} - reflectance of the atmosphere (value of 0.03) according to [21] and [23] and τ_{sw} - atmospheric transmissivity at the instant of the satellite passage [1].

The surface temperature was estimated from the emissivity in the spectral domain of the thermal band, using the spectral radiance (L_b , $W m^{-2} sr^{-1} \mu m^{-1}$) of the Landsat-8 sensor TIRS thermal band 10, eq. (9) [2]. It is worth noting that the temperature was converted from Kelvin (K) to

degrees Celsius ($^{\circ}C$).

$$T_s = \frac{K_2}{\left(\frac{\epsilon_{NB} \times K_1}{L_b} + 1\right)} \quad (9)$$

where: T_s - surface temperature ($^{\circ}C$); ϵ_{NB} - thermal band spectral emissivity; K_1 and K_2 - thermal band calibration constants for the TIRS sensor of $774.89 W m^{-2} sr^{-1} \mu m^{-1}$ and $1321.08 K$, respectively, extracted from the metadata of the processed images.

2.4. Statistical analysis

2.4.1. Descriptive statistic

The main results and differences of micrometeorological biophysical parameters relative to the local climate of the semiarid region and also to anthropic activities were evaluated by descriptive statistics, as measures of central tendency (mean) and dispersion (minimum and maximum, standard deviation - SD and coefficient of variation - CV).

2.4.2. Thematic variability

The thematic maps of vegetation indexes, albedo, and surface temperature were also evaluated by their spatial-temporal variability observing the values of the coefficient of variation (CV, %), where $CV < 12\%$ - represents low variability; $12\% < CV < 60\%$ - medium variability; and $CV > 60\%$ - high variability [26].

3. Results and discussion

The spatial-temporal monitoring presents the behavior pattern of the thematic maps of the vegetation indices (NDVI, SAVI, and LAI) and the albedo and surface temperature parameters. It was mainly highlighting the variability of both biophysical parameters, since the region has different uses and occupations of the soil, with the agricultural area, water bodies, urban area, and native vegetation of the Caatinga.

Fig. 2 illustrates the thematic maps of the NDVI vegetation index from 2013 to 2018, which ranged from -1.00 to 0.87, showing its spatial-temporal distribution in the different land uses and occupations of the semiarid region of Pesqueira, Pernambuco.

The NDVI maps were strongly linked to local rainfall, mainly in the rainy season. And when in the dry season, the vegetation of the Caatinga biome highlighted thematic maps losing its leaf condition to avoid transpiration in periods of water scarcity [8,22].

Analyzing the NDVI for the year 2013, it can be observed that the absence of rain in the rainy season itself (Fig. 2A) presents a large percentage of area with pixels in the orange color, evidencing that the vegetation coverage is with less intensity or even in a situation of exposed soil, a fact also evidenced in the dry season (Fig. 2B), a similarity that can be verified by the average of pixels, which accounted for values

of 0.33 for the two periods. It is worth mentioning that the anthropic action can also negatively influence this index, considering that the environmental deforestation and the burning reduce the vegetation coverage.

The NDVI for the year 2015, although being a dry year with a total annual rainfall below the local historical average (according to Table 1), shows a clear difference between the maps of the rainy season (Fig. 2C) and dry (Fig. 2D). This differentiation is because the vegetation characteristic of the Caatinga has rapid responses to climate change, and therefore can recover its leaves with the first precipitation.

Taking into account the accumulated rainfall in the 90 days preceding the date the satellite passed (Table 2), we have a rainfall volume of 86 mm, which was able to change the vegetation coverage scenario to the first image in 2015, reaching an average NDVI of 0.44 (Table 3). However, the second image of the same year had a total accumulated rainfall in the 90 days before the acquisition of the image of only 12.4 mm (Table 2), which caused the leaves to be lost as a response to the water scarcity and consequently increased evapotranspiration, justifying the average NDVI of 0.28 (Table 3) for the second period, giving the difference in the color of pixels for the two images of the year 2015 (Figs. 2C and 2D).

For the year 2018, the NDVI thematic maps show that during the rainy season (Fig. 2E), this index reached the closest values to 1 (dark blue pixels) for all six images. In fact, for this period, there was intense rainfall in the 90 days before the image capture, reaching an accumulated 240 mm (Table 2), so that the vegetation cover could expand and avoid soil exposure, also reaching an NDVI average of 0.67 (Table 3). In the dry season image (Fig. 2F), there is a reduction in areas with dark blue pixels, but it does not reach a situation of values very close to zero, i.e., exposed soil. This is because, even though it is considered a dry period, the accumulation of rainfall for the 90 days before the image acquisition was 79.4 mm (Table 2); that is, despite the disparity of rainfall with the rainy period, the dry season was not as intense as in other years, providing a volume of rain capable of maintaining the vegetation cover and preventing the soil from being exposed, with the average NDVI for this period of 0.33 (Table 3).

Fig. 3 illustrates the thematic maps of the SAVI vegetation index between the years 2013 and 2018, with values ranging between -0.19 and 0.78, highlighting its spatial-temporal distribution in the different land uses of the semiarid region, which according to [2], this index is more specifically a biomass indicator.

The SAVI can transmit more easily the changes that have occurred on the surface of the areas under study because it can have a spectral response of the vegetation with the "background" effects of the soil softened [20]. The SAVI brings in its thematic maps a greater approximation of the reality of local vegetation coverage, especially during periods of drought, which was also observed in other studies [19,22].

The interpretations of the SAVI maps are similar to the

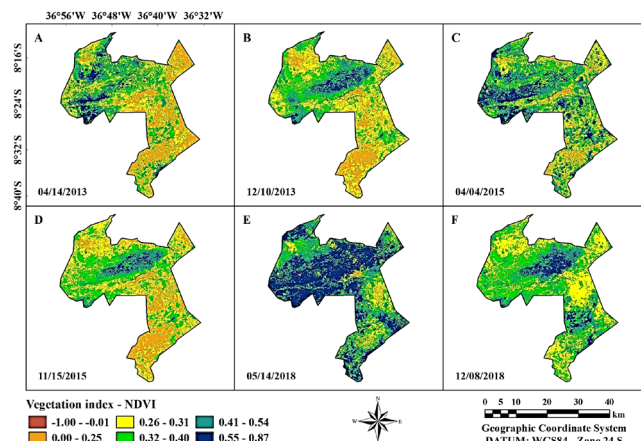


Figure 2. Spatial-temporal distribution of NDVI vegetation index in the rainy season: 04/14/2013 (A); 04/04/2015 (C); 05/14/2018 (E) and in the dry season: 10/12/2013 (B); 11/15/2015 (D); 12/08/2018 (F). Source: The Authors.

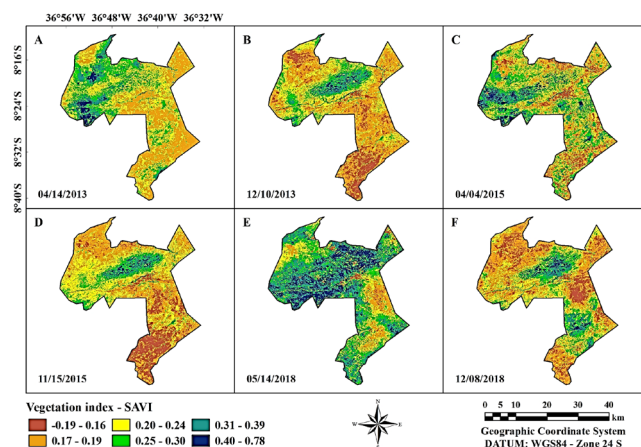


Figure 3. Spatial-temporal distribution of the SAVI vegetation index in the rainy season: 04/14/2013 (A); 04/04/2015 (C); 05/14/2018 (E) and in the dry season: 10/12/2013 (B); 11/15/2015 (D); 12/08/2018 (F). Source: The Authors

NDVI because, as previously cited, both deal with plant cover, but differing by the fact that the SAVI has a soil adjustment factor, which consequently can bring closer to the reality. To minimize the effects of the soil, it can be seen that for 2013, the image of the rainy season (Fig. 3A) has higher SAVI values than the dry season (Fig. 3B), where the first recorded an average of 0.22 and the second in the 0.20 (Table 2), different from what occurred in the NDVI, where both periods obtained the same averages. The SAVI shows itself as the best method for determining vegetation cover in the Brazilian semiarid region since the NDVI can show values altered by the effects of the soil.

With the same thought above, it is observed that the year 2015 has SAVI values even more worrying in the dry season (Fig. 3C), even being a year with an average annual rainfall below normal, the rains preceding the periods of the capture of images was enough to obtain less worrying values, a greater amount of vegetation cover and less susceptible to

environmental degradation processes in the region, in the period of rainfall (Fig. 3D). According to Table 3, the SAVI average for the rainy season was 0.27, while for the dry season, it was 0.19, which justifies the appearance of red pixels, representing areas of exposed soil and/or with little vegetation.

In the year 2018, due to the greater amount of rainfall (Fig. 3E), pixels with intense green and blue coloration can be observed, a vegetation cover with large proportions, and an average SAVI of 0.43 (Table 3). However, when the period of drought arrives (Fig. 3F), it was verified that the intense vegetation gives way to areas with little or no vegetation cover, which is a reflection of the mechanisms adopted by the Caatinga to minimize the effects of drought in the semiarid region through the loss of its leaves, directly diminishing the average of the SAVI index to the value of 0.21 (Table 3).

Fig. 4 also illustrates the thematic maps of the leaf area index - LAI that highlights the spatial-temporal monitoring of this index with a variation in vegetation values between 0.00 and 6.00 $\text{m}^2 \text{m}^{-2}$.

It can be seen that for the map of April 14th, 2013 (Fig. 4A), due to the delay in rainfall, the LAI had values close to or equal to zero, with a very low average of 0.25 $\text{m}^2 \text{m}^{-2}$ for the entire region of Pesqueira (Table 3), indicating that the vegetation cover gave way to the exposed soil areas. In the dry season of the same year (Fig. 4B), the situation is even more worrying due to the increase in orange and red pixels, and consequently, the decrease in green, which can be seen by the reduction of the average LAI (0.22 $\text{m}^2 \text{m}^{-2}$) (Table 3).

For the year 2015, in the rainy period (Fig. 4C), it can be seen that even if there is an intense coloring of pixels with orange and red areas, this period has a higher average of LAI when compared to the dry period of the same year (Fig. 4D), with the respective averages 0.40 and 0.18 $\text{m}^2 \text{m}^{-2}$ (Table 3). It is worth remembering that this is a year with a lower than expected annual rainfall average. Therefore, its dry period was even more critical than that of 2013, which suffered the climatic disturbances coming from El Niño.

For the year 2018, it was observed that due to rainfall regularly occurring during the rainy season, the LAI of this period (Fig. 4E) obtained outstanding values, with most of the region presenting good results of the leaf area, with the overall average being 0.98 $\text{m}^2 \text{m}^{-2}$ (Table 3). During the dry season, LAI decreased again, which is already expected since the local biome has fast responses to climate variability in the semiarid region. Thus, the average LAI decreased to 0.23 $\text{m}^2 \text{m}^{-2}$ (Table 3). On the other hand, it is also worth mentioning the interference of anthropic activities, considering that both deforestation and burning for the expansion of agriculture and cattle raising have the potentials of environmental degradation and, consequently, the reduction of vegetation coverage and leaf area in the semiarid regions of Brazil [22,23].

Table 3 highlights the statistical behavior and variability of the NDVI, SAVI and LAI vegetation indices in the semiarid region of Pesqueira.

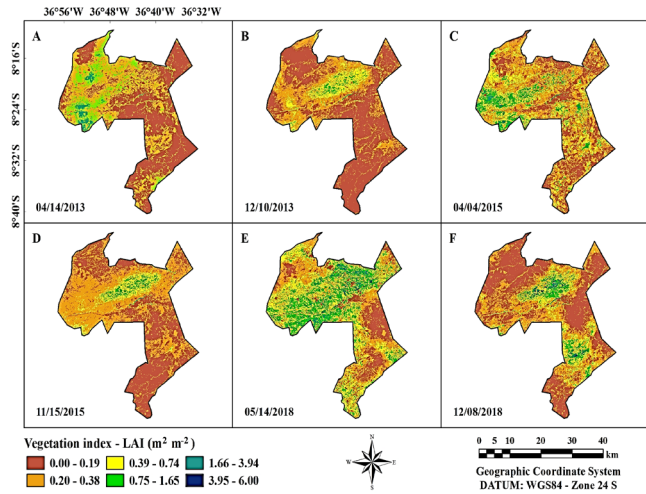


Figure 4. Spatial-temporal distribution of the LAI vegetation index in the rainy season: 04/14/2013 (A); 04/04/2015 (C); 05/14/2018 (E) and in the dry season: 10/12/2013 (B); 11/15/2015 (D); 12/08/2018 (F). Source: The Authors.

Table 3.

Statistical analysis and spatial-temporal variability of the NDVI, SAVI and LAI vegetation indices in the semiarid region of Pesqueira, Pernambuco, Brazil.

| Vegetation index - NDVI | | | | | |
|-------------------------------------------------------|---------|---------|---------|------|--------|
| Image date | Minimum | Maximum | Average | SD | CV (%) |
| 04/14/2013 | -0.87 | 0.85 | 0.33 | 0.13 | 39.39 |
| 10/12/2013 | -0.62 | 0.86 | 0.33 | 0.10 | 30.30 |
| 04/04/2015 | -1.00 | 0.86 | 0.44 | 0.13 | 29.54 |
| 11/15/2015 | -0.67 | 0.86 | 0.28 | 0.09 | 32.14 |
| 05/14/2018 | -1.00 | 0.87 | 0.67 | 0.14 | 20.89 |
| 12/08/2018 | -0.70 | 0.82 | 0.33 | 0.11 | 33.33 |
| Vegetation index - SAVI | | | | | |
| 04/14/2013 | -0.15 | 0.71 | 0.22 | 0.07 | 31.81 |
| 10/12/2013 | -0.20 | 0.76 | 0.20 | 0.06 | 30.00 |
| 04/04/2015 | -0.17 | 0.74 | 0.27 | 0.07 | 25.92 |
| 11/15/2015 | -0.14 | 0.78 | 0.19 | 0.05 | 26.31 |
| 05/14/2018 | -0.17 | 0.76 | 0.43 | 0.10 | 23.25 |
| 12/08/2018 | -0.17 | 0.69 | 0.21 | 0.06 | 28.57 |
| Vegetation index - LAI ($\text{m}^2 \text{m}^{-2}$) | | | | | |
| 04/14/2013 | 0.00 | 6.00 | 0.25 | 0.20 | 80.00 |
| 10/12/2013 | 0.00 | 6.00 | 0.22 | 0.18 | 81.81 |
| 04/04/2015 | 0.00 | 6.00 | 0.40 | 0.21 | 52.50 |
| 11/15/2015 | 0.00 | 6.00 | 0.18 | 0.14 | 77.77 |
| 05/14/2018 | 0.00 | 6.00 | 0.98 | 0.46 | 46.93 |
| 12/08/2018 | 0.00 | 6.00 | 0.23 | 0.17 | 73.91 |

Source: The Authors.

The results of the thematic maps of the NDVI and SAVI vegetation indices, for example, presented a spatial-temporal behavior of medium variability, with CV varying between 23.25 and 39.39% (Table 3). The LAI index, although presenting the same behavior in some images, highlighted mostly high variability behavior (Table 3). This behavior is common for these parameters in studies performed in semiarid regions, corroborating mainly with the variabilities founded by [22], which varied from 35 to 57% (mean variability) for the SAVI index and high variability for LAI. This reinforces that the region presents different uses and occupations of the soil, such as areas of agricultural activities,

rivers, reservoirs, urban areas, and especially the areas of vegetation of Caatinga thin and dense, in addition to degraded areas and exposed soil.

Fig. 5 illustrates the spatial-temporal variability of the surface albedo, which varied from 0.01 to 0.69. According to the variations in pixel cover tonality, it is possible to assign the different types of land use and occupation, as well as environmental changes to the territorial limit of the municipality of Pesqueira. The spatial-temporal analysis of the albedo aims to provide better support to verify and identify more accurately the areas with environmental changes in the semiarid region, confirming mainly the analyses highlighted in the vegetation indexes NDVI, SAVI, and LAI.

From the thematic maps of the surface albedo for 2013, there is a substantial similarity between Figs. 5A and 5B, which can be proved by the average of the pixel values in Table 4. This similarity is due to the previous year of 2012, when the El Niño phenomenon occurred and which directly caused a climatic derangement throughout the semiarid region of Brazil, mainly to the absence of rainfall and severe water deficit in the first months of the year, where the heaviest rain is expected especially in the study region. The year 2013 can be treated as an atypical year, where the rainy season that should receive more rainfall presented spectral responses very close to those recorded in the dry period.

It is also worth noting that although 2013 has the highest annual average rainfall (510.8 mm, Table 1), rainfall was concentrated between the second half of April and early August, that is, outside the rainy season. The rains came after the date of the capture of the image of 04/14/2013 (Fig. 5A) and stopped before the capture of the image of 04/04/2015 (Fig. 5C), causing this year to have an anomaly in the distribution of rains, a fact that can be explained by the interference of El Niño.

In 2015, a similarity between the rainy period (Fig. 5C) and the dry period (Fig. 5D) can be seen. The fact is that this year was characterized as a year of drought with rainfall below the annual average (335.7 mm, Table 1). It is possible to observe that the albedo values remained high in the central, eastern, and southern parts of the municipality. These numbers correspond to low humidity or even the absence of water bodies.

Figs. 5E and 5F showed a significant difference between the rainy and dry seasons, respectively, for the year 2018. This year was considered a typical year, which rains occur between February and May, the remaining months being the dry season. The spectral response to albedo in the dry season of 2018 is of low numbers because the presence of water bodies and even the surface humidity can absorb more solar radiation and have a low reflectivity, which does not happen in the dry period, since the exposed soil or the low moisture existing in the site is not able to absorb the radiation, which provides a high reflectivity which results in high values of albedo.

Fig. 6 shows the thematic maps of spatial-temporal surface temperature variability, which, like albedo and

vegetation indices, has a link with local precipitation. This relationship can be explained by the fact that when there is rain, the vegetation recovers its leaves more quickly. Thus there is an expansion of vegetation cover, which prevents or at least minimizes exposure of exposed soil in the region. In this context, it is expected that the covered soils will have milder temperatures than those that are exposed since the vegetation will protect it from solar radiation.

As previously observed, the rainy and dry periods of the year 2013 are quite similar. For this reason, the surface temperature for these periods obtained a small variance, being, in the rainy season, the average of 36.47 °C, while the dry season, 37.13 °C (Table 4).

In 2015, despite being the year with the lowest annual average rainfall, it was noted that there is an increase in temperature in the dry season when compared to the rainy season. This occurs because the rains, even being of low intensity, were concentrated in a single period. The rain can promote the developing of the vegetation cover and protecting the surface from solar radiation, reaching an average temperature for this period of 32.92 °C, while in the dry period, this average rose to 39.73 °C (Table 4).

Finally, in 2018 was within normality, the annual average rainfall was consistent with the locality, and rainfall was generally concentrated during the rainy season, which recorded an average surface temperature of 26.30 °C and for the dry period of the same year, an average of 36.42 °C (Table 4).

Table 4 highlights the statistical behavior and variability of biophysical parameters, albedo and surface temperature in the semiarid region of Pesqueira.

As previously observed, the rainy and dry periods of the year 2013 are quite similar. For this reason, the surface temperature for these periods obtained a small variance, being, in the rainy season, the average of 36.47 °C, while the dry season, 37.13 °C (Table 4).

In 2015, despite being the year with the lowest annual average rainfall, it was noted that there is an increase in temperature in the dry season when compared to the rainy season. This occurs because the rains, even being of low intensity, were concentrated in a single period. The rain can promote the developing of the vegetation cover and protecting the surface from solar radiation, reaching an average temperature for this period of 32.92 °C, while in the dry period, this average rose to 39.73 °C (Table 4).

Finally, in 2018 was within normality, the annual average rainfall was consistent with the locality, and rainfall was generally concentrated during the rainy season, which recorded an average surface temperature of 26.30 °C and for the dry period of the same year, an average of 36.42 °C (Table 4).

Table 4 highlights the statistical behavior and variability of biophysical parameters, albedo and surface temperature in the semiarid region of Pesqueira.

From the results of the thematic maps of albedo and surface temperature, a spatial-temporal behavior of medium and high variability was observed, respectively, with CV

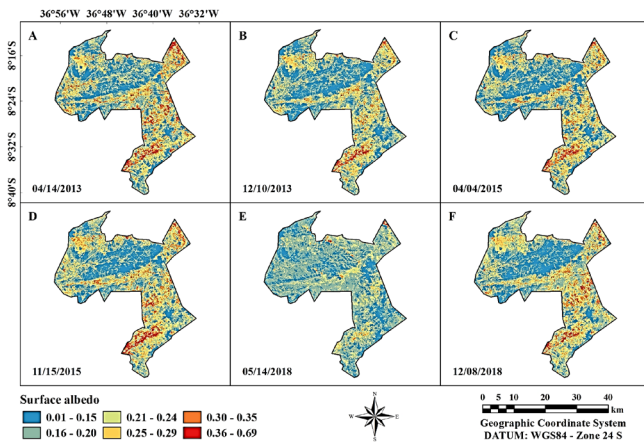


Figure 5. Spatial-temporal distribution of surface albedo in the rainy season: 04/14/2013 (A); 04/04/2015 (C); 05/14/2018 (E) and in the dry season: 10/12/2013 (B); 11/15/2015 (D); 12/08/2018 (F). Source: The Authors.

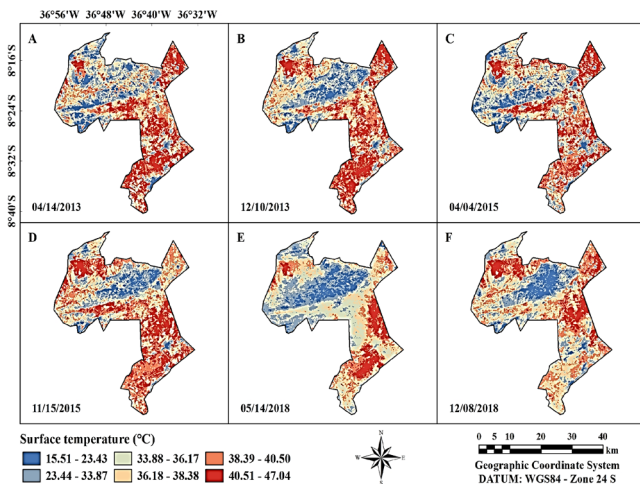


Figure 6. Spatial-temporal distribution of surface temperature in the rainy season: 04/14/2013 (A); 04/04/2015 (C); 05/14/2018 (E) and the dry season: 10/12/2013 (B); 11/15/2015 (D); 12/08/2018 (F). Source: The Authors.

Table 4.

Statistical analysis and spatial-temporal variability of the albedo and surface temperature parameters in the semiarid region of Pesqueira, Pernambuco, Brazil.

| Surface albedo | | | | | |
|--------------------------|-------|-------|-------|------|-------|
| 04/14/2013 | 0.02 | 0.47 | 0.21 | 0.06 | 28.57 |
| 10/12/2013 | 0.03 | 0.40 | 0.19 | 0.05 | 26.31 |
| 04/04/2015 | 0.01 | 0.46 | 0.20 | 0.06 | 30.00 |
| 11/15/2015 | 0.05 | 0.69 | 0.25 | 0.07 | 28.00 |
| 05/14/2018 | 0.01 | 0.42 | 0.15 | 0.04 | 26.66 |
| 12/08/2018 | 0.04 | 0.48 | 0.22 | 0.06 | 27.27 |
| Surface temperature (°C) | | | | | |
| 04/14/2013 | 25.25 | 44.35 | 36.49 | 3.21 | 8.79 |
| 10/12/2013 | 24.50 | 47.04 | 37.13 | 3.53 | 9.50 |
| 04/04/2015 | 20.62 | 40.78 | 32.92 | 2.92 | 8.86 |
| 11/15/2015 | 26.14 | 47.98 | 39.73 | 3.45 | 8.68 |
| 05/14/2018 | 15.51 | 36.10 | 26.30 | 2.45 | 9.31 |
| 12/08/2018 | 25.33 | 46.11 | 36.42 | 3.30 | 9.06 |

Source: The Authors.

varying between 26.31 and 30.00% for albedo, and between 8.68 and 9.50% for temperature (Table 4). It is also a common behavior for these parameters in semiarid regions, according to the variabilities found by [23].

4. Conclusions

Vegetation indexes are good indicators of the processes of environmental degradation and/or recovery of Caatinga vegetation cover in the Brazilian semiarid region. They can identify the areas most susceptible to degradation and desertification since exposed soils tend to suffer erosion and, consequently, the destruction of entire areas.

The SAVI proved to be the most appropriate for the observation of the Caatinga biome because the semiarid regions are endowed with a vegetation cover capable of rapidly losing their leaves in water scarcity, which allows the exposure of soil that in other indexes, such as the NDVI, can disturb reflectivity and give overestimated responses of vegetation cover, not consistent with local reality.

The environmental changes in vegetation in both seasons reveal that this type of spatial-temporal monitoring is essential for the conservation of the Caatinga biome in the semiarid regions of Brazil since remote sensing techniques with satellite images are capable of operating in large areas practically and efficiently, in a short period and at a low cost, facilitating decision making and consequently acting to mitigate environmental degradation and soil desertification.

Acknowledgements

We would like to thank the Fundação de Amparo à Ciência e Tecnologia do Estado de Pernambuco (FACEPE IBPG-0307-5.03/19) and the Coordenação de Aperfeiçoamento de Pessoal de Nível Superior (CAPES, Brazil) - Finance Code 001 by the granting of doctoral scholarships. The INMET by the availability of weather surface data and NASA/USGS by the free availability of the satellite images.

References

- [1] Allen, R.G., Tasumi, M. and Trezza, R., Satellite-Based energy balance for mapping evapotranspiration with internalized calibration (METRIC) - Model. *Journal of Irrigation and Drainage Engineering*, 133(4), pp. 380-394, 2007. DOI: 10.1061/(ASCE)0733-9437(2007)133:4(380)
- [2] Allen, R.G., Tasumi, M., Trezza, R., Bastiaanssen, W.G.M., SEBAL (Surface Energy Balance Algorithms for Land) - Advance training and user's Manual-Idaho Implementation. 2002, 97 P.
- [3] Alvares, C.A., Stape, J.L., Sentelhas, P.C., Moraes, G., Leonardo, J. and Sparovek, G., Köppen's climate classification map for Brazil. *Meteorologische Zeitschrift*, 22(6), pp. 711-728, 2013. DOI: 10.1127/0941-2948/2013/0507
- [4] APAC - Agência Pernambucana de Águas e Clima. Hydrographic Basins. [online]. [Access: November 30, 2019]. Available at: <http://www.apac.pe.gov.br/meteorologia/monitoramento-pluvio.php#>
- [5] Araújo, F.S., Rodal, M.J.N., Barbosa, M.R.V. and Martins, F.R., Repartição da flora lenhosa no domínio da caatinga. In: Araújo, F.S., Rodal, M.J.N., Barbosa, M.R.V. (Org.). *Análise das variações da biodiversidade do bioma caatinga: suporte a estratégias regionais de conservação*. Ministério do Meio Ambiente, Secretaria de Biodiversidade e Florestas, Biodiversidade, 12, Brasília, DF, Brasil, 2005. pp. 16-33.

- [6] Arraes, F.D., Andrade, E.M. and Silva, B.B., Dinâmica do balanço de energia sobre o açude Orós e suas adjacências. *Caatinga Magazine*, [online]. 25(1), pp. 119-127, 2012. Available at: <https://www.redalyc.org/articulo.oa?id=237123860018>
- [7] Bastiaanssen, W.G.M., SEBAL-based sensible and latent heat fluxes in the irrigated Gediz Basin, Turkey. *Journal of Hydrology*, 229(1-2), pp. 87-100, 2000. DOI: 10.1016/S0022-1694(99)00202-4.
- [8] Bezerra, J.M., Moura, G.B., Silva, B.B., Lopes, P.M., Silva, Ê.F.F., Parâmetros biofísicos obtidos por sensoriamento remoto em região semiárida do estado do Rio Grande do Norte, Brasil. *Revista Brasileira de Engenharia Agrícola e Ambiental*, 18(1), pp. 73-84, 2014. DOI: 10.1590/s1415-43662014000100010
- [9] CGEE - Centro de Gestão e Estudo Estratégicos. The issue of water in the Northeast in year 2016. [online]. [Access: August 25th of 2020]. Available at: <https://www.cgee.org.br/home>
- [10] Chander, G., Markham, B.L. and Helder, D.L., Summary of current radiometric calibration coefficients for Landsat MSS, TM, ETM+, and EO-1 ALI sensors. *Remote Sensing of Environment*, 113(5), pp. 893-903, 2009. DOI: 10.1016/j.rse.2009.01.007
- [11] Santos, H.G., Jacomine, P.K.T., Anjos, L.H.C., Oliveira, V.A., Lumberreras, J.F., Coelho, M.R., Almeida, J.A., Araujo Filho, J.C., Oliveira, J.B. and Cunha, T.J.F., Brazilian soil classification system. *Embrapa Solos*, 5th ed., EMBRAPA, Brasília, DF, Brasil, 2018. 516 P.
- [12] Huete, A.R., A soil-adjusted vegetation index (SAVI). *Remote Sensing of Environment*, 25(3), pp. 295-309, 1988. DOI: 10.1016/0034-4257(88)90106-X
- [13] IBGE - Instituto Brasileiro de Geografia e Estatística. Geosciences. Brazilian semiarid. [online]. [Access: August 25, 2020]. Available at: <https://www.ibge.gov.br/geociencias/cartas-e-mapas/mapas-regionais/15974-semiarido-brasileiro.html?=&t=o-que-e>
- [14] INMET - Instituto Nacional de Meteorologia. Weather data: Weather database - Annual historical data. [online]. [Access: November 31, 2019]. Available at: <https://portal.inmet.gov.br/dadoshistoricos>
- [15] IQBAL, M., An introduction to solar radiation. Academic Press., London, UK, 1983, 390 P.
- [16] LAPIS/UFAL. Satellite Image Analysis and Processing Laboratory/ Federal University of Alagoas. Climate change: 10 impacts on Caatinga. [online]. LAPIS/UFAL, 2019. [Access: November 26, 2019]. Available at: <https://www.letrasambientais.com.br/posts/mudancas-climaticas-10-impactos-sobre-a-caatinga>.
- [17] Montenegro, A.A. and Montenegro, S.M.G.L., Variabilidade espacial de classes de textura, salinidade e condutividade hidráulica de solos em planície aluvial. *Revista Brasileira de Engenharia Agrícola e Ambiental*, 10(1), pp. 30-37, 2006. DOI: 10.1590/S1415-43662006000100005
- [18] Montenegro, A.A.A. and Ragab, R., Hydrological response of a Brazilian semiarid catchment to different land use and climate change scenarios: modelling study. *Hydrological Processes*, 24(19), pp. 2705-2723, 2010. DOI: 10.1002/hyp.7825
- [19] Oliveira, J.D.A., Medeiros, B.C., Silva, J.L.B., Moura, G.B.A., Lins, F.A.C., Nascimento, C.R. and Lopes, P.M.O., Space-temporal evaluation of biophysical parameters in the High Ipanema watershed by remote sensing. *Journal of Hyperspectral Remote Sensing*, 7(6), pp. 357-366, 2017. DOI: 10.29150/jhrs.v7.6.p357-366
- [20] Ribeiro, E.P., Nóbrega, R.S., Mota Filho, F.O. and Moreira, E.B., Estimativa dos índices de vegetação na detecção de mudanças ambientais na bacia hidrográfica do rio Pajeú. *Geosul*, 31(62), pp. 59-92, 2016. DOI: 10.5007/2177-5230.2016v31n62p59
- [21] Silva, B.B.D., Braga, A.C., Oliveira, L.M., Montenegro, S.M. and Barbosa Junior, B., Procedures for calculation of the albedo with OLI-Landsat 8 images: application to the Brazilian semiarid. *Revista Brasileira de Engenharia Agrícola e Ambiental*, 20(1), pp. 3-8, 2016. DOI: 10.1590/1807-1929/agriambi.v20n1p3-8.
- [22] Silva, J.L.B., Moura, G.B.A., Silva, Ê.F.F., Lopes, P.M.O., Silva, T.T.F., Lins, F.A.C., Silva, D.A.O. and Ortiz, P.F.S., Spatial-temporal dynamics of the Caatinga vegetation cover by remote sensing in municipality of the Brazilian semi-arid. *Revista Brasileira de Ciências Agrárias*, 14(4), pp. 1-10, 2019. DOI: 10.5039/agraria.v14i4a7128
- [23] Silva, J.L.B., Moura, G.B.A., Lopes, P.M.O., Silva, Ê.F.F., Ortiz, P.F.S., Silva, D.A.O., Silva, M.V. and Guedes, R.V.S., Spatial-temporal monitoring of the risk of environmental degradation and desertification by remote sensing in a Brazilian semiarid region. *Revista Brasileira de Geografia Física*, 13(02), pp.544-563, 2020. DOI: 10.26848/rbgf.v13.2.p544-563
- [24] Silva, L.G. and Galvêncio, J.D., Análise Comparativa da Variação nos Índices NDVI e SAVI no Sítio PELD – 22, em Petrolina – PE, na Primeira Década do Século XXI. *Revista Brasileira de Geografia Física*, 5(6), pp. 1446-1456, 2012. DOI: 10.26848/rbgf.v5.6.p1446-1456
- [25] Thorntwaite, C.W., Na approach toward a rational classification of climate. *Geographical Review*. New York, [online]. 38(1), pp.55-94, 1948. Available at: <https://www.jstor.org/stable/210739>
- [26] Warrick, A.W. and Nielsen, D.R., Spatial variability of soil physical properties in the field. In: Hillel, D., Ed., *Applications of soil physics*. Academic Press. New York, USA, 1980. pp. 319-344.
- [27] Xavier, R.A., Maciel, J.S.I and Silva, V.M.A., Análise espacial das chuvas na bacia do rio Taperoá, Região Semiárida da Paraíba. *Brazilian Journal of Physical Geography*, 09(05), pp. 1357-1369, 2016. DOI: 10.26848/rbgf.v9.5.p1357-1369

J.A.M. Rodrigues, is BSc. Eng. in Agricultural and Environmental Engineering in 2015 from the Federal Rural University of Pernambuco (UFRPE), Brazil. MSc. in Agricultural Engineering in 2019 from UFRPE. Currently a PhD student in Agricultural Engineering at UFRPE, Brazil. ORCID: 0000-0002-1340-7227

P.M.O. Lopes, is BSc. of Meteorology in 1997 from the Federal University of Campina Grande (UFCG), Brazil. Graduated in Physics in 1999 from the State University of Paraíba (UEPB), Brazil. MSc. in Meteorology in 1999 from UFCG. PhD in Remote Sensing, in 2006 from the National Institute for Space Research (INPE), Brazil. Currently associate professor at Federal Rural University of Pernambuco (UFRPE), Brazil. ORCID: 0000-0002-6632-4062

J.L.B. Silva, is Technologist in Irrigation and Drainage, in 2014 from the Federal Institute of Ceará (IFCE), Campus Iguatu, Ceará, Brazil. MSc. in Agricultural Engineering in 2016 from the Federal Rural University of Pernambuco (UFRPE), Brazil. Currently a PhD student in Agricultural Engineering at UFRPE, Brazil. ORCID: 0000-0002-2611-4036.

H.L. Araújo, is BSc. Eng. in Agricultural Engineering in 2015, from the State University of Goiás (UEG), Brazil. MSc. in Agricultural Engineering in 2019 from Federal Rural University of Pernambuco (UFRPE), Brazil. ORCID: 0000-0001-5762-519X.

M.V. Silva, is BSc. Eng. in Agricultural Engineering in 2016, from the State University of Goiás (UEG), Brazil. MSc. in Agricultural Engineering in 2019 from the Federal Rural University of Pernambuco (UFRPE). Currently a PhD student in Agricultural Engineering at UFRPE, Brazil. ORCID: 0000-0002-1318-2320.

A. Santos, is BSc. in Agronomy in 2016, from the Federal University of Alagoas (UFAL), Brazil. MSc. in Agriculture and Environment in 2018, from the UFAL, Brazil. Currently a PhD student in Agricultural Engineering at Federal Rural University of Pernambuco (UFRPE), Brazil. ORCID: 0000-0001-7195-4520.

P.H.D. Batista, is Technologist in Irrigation and Drainage in 2015, from the Federal Institute of Ceará (IFCE), Campus Iguatu, Ceará, Brazil. MSc. in Agricultural Engineering in 2017, from the Federal Rural University of Pernambuco (UFRPE), Brazil. Currently a PhD student in Agricultural Engineering at UFRPE, Brazil. ORCID: 0000-0002-8710-5678.

G.B.A. Moura, is BSc. in Meteorology in 1990, from the Federal University of Campina Grande (UFCG), Brazil, MSc. in 1993 in Meteorology from the UFCG. PhD in 2001 in Oceanography from the Federal University of Pernambuco (UFPE), Brazil. Currently is full professor at Federal Rural University of Pernambuco (UFRPE), Brazil. ORCID: 0000-0001-9073-8145.